MECHANICS AND ANALYSIS OF FABRIC COMPOSITES AND STRUCTURES

Evgeny V. Morozov

School of Mechanical Engineering, University of Natal
Durban 4041, South Africa
E-mail: morozov@nu.ac.za

Abstract

This paper is devoted to the mechanics, modelling and analysis of fabric-reinforced composites and structural components. A theoretical and experimental characterisation of elastic properties of the textile composites is considered. Typical stress-strain diagrams for fibreglass fabric composites and composites reinforced with knitted fabrics loaded in tension at different angles are presented. The special case of the three-dimensional reinforcement structure of composite material, composed of spatially-oriented fabric layers is discussed and corresponding models considered. Manufacturing technology for such structures includes a three-dimensional lay-up process in which the specially designed fabric patterns are placed onto the mould or mandrel. The implementation of the material model is illustrated with results of the stress-strain analysis of thin-walled spatially reinforced structural components.

Key words:

fabric composites, experimental characterisation, spatially reinforced composite components

1. INTRODUCTION

Composite materials reinforced with woven, braided and knitted fabrics are becoming increasingly popular for various structural applications in the automotive, aerospace, and other industrial sectors. Typical processing techniques include variations of lay-up manufacturing and contact lamination technologies, resin transfer moulding, vacuum/pressure bag moulding and autoclaving of fabric based thermosetting prepregs, and compression/preform moulding of thermoplastic and thermosetting composites.

The purpose of this paper is to discuss the developments in the modelling and characterisation of fabric reinforced composite materials and structural components and to demonstrate for particular applications (spatially fabric-reinforced thin-walled structures) how it is possible to combine the basic advantages of fabric composites with those provided by implementation of three-dimensional reinforcement orientation in order to develop efficient designs of lightweight thin-walled composite components. The shape and geometry of the structural components under consideration reasonably implies an application of the approaches developed for thin-walled plates and shells. At the same time, analysis of the three-dimensional stress state of composite material at the level of elementary layers is essential in order to provide a structural integrity of the part at the stages of design and manufacture. The current paper demonstrates an application of corresponding approaches to the analysis of thin-walled composite shells of revolution with spatial orientation of fabric reinforcement. The particular geometry and material structure of the shell reinforced with carbon fabric patterns have been used as an example of the application of the general approach.

2. FABRIC REINFORCEMENT

Textile preforming plays an important role in composite technology providing glass, aramid, carbon, and hybrid fabrics that are widely used as reinforcing materials. The main advantages of woven composites are their cost efficiency and high processability, particularly in lay-up manufacturing of large-scale structures. At the same time, bending of fibres in the process of fabric weaving results in substantial reduction of material strength and stiffness. As can be seen in Figure 1, where a typical

woven structure is shown the warp (lengthwise) and fill (crosswise) yarns forming the fabric make the angle $\alpha \geq 0$ with the plane of the fabric layer.

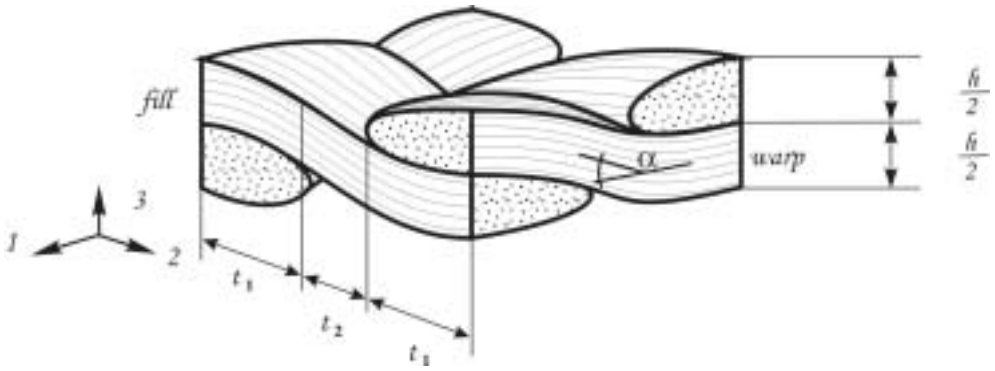

Figure 1. Elementary cell of a fabric structure

A demonstration of how the angle α affects the stiffness of the composite materials reinforced with the fabric layers has been presented in [1]. The tensile loading of the structural cell shown in Figure1 in the warp direction has been considered. An apparent modulus of elasticity was expressed in terms of the moduli of the warp yarns, E_w, and fill yarns, E_f, as follows

$$E_a = (E_f A_f + E_w A_w)/A_a \tag{1}$$

Here $A_a = h(2t_1 + t_2)$ is the apparent cross-sectional area and

$$A_f = h(2t_1 + t_2)/2 \qquad A_w = h(4t_1 + t_2)/4$$

are the areas of the fill and warp yarns in the cross section (see Figure 1). Substitution into equation (1) yielded

$$E_a = \frac{E_f}{2} + \frac{E_w(4t_1 + t_2)}{4(2t_1 + t_2)} \tag{2}$$

Since the fibres of the fill yarns are orthogonal to the loading direction (axis 1 in Figure1), the modulus of the fill yarn material could be taken as $E_f = E_2$, where E_2 is the transverse modulus of a unidirectional composite reinforced with the same fibres. Compliance of the warp yarn can be decomposed into two parts corresponding to t_1 and t_2 in Figure1, i.e.

$$\frac{2t_1 + t_2}{E_w} = \frac{2t_1}{E_1} + \frac{t_2}{E_a} \tag{3}$$

Here, E_1 is the longitudinal modulus of a unidirectional composite, while E_α can be determined with the aid of the following equation, derived in [1] for the unidirectional anisotropic layer

$$\frac{1}{E_\alpha} = \frac{\cos^4\alpha}{E_1} + \frac{\sin^4\alpha}{E_2} + \left(\frac{1}{G_{12}} - \frac{2\nu_{21}}{E_1}\right)\sin^2\alpha\cos^2\alpha \tag{4}$$

Replacement of $1/E_a$ in equation (3) with its expression from equation (4) and subsequent substitution of the resulting fraction $E_w/(2t_1 + t_2)$ into equation (2) yields

$$E_a = \frac{E_2}{2} + \frac{E_1(4t_1 + t_2)}{4\{2t_1 + t_2[\cos^4\alpha + \frac{E_1}{E_2}\sin^4\alpha + (\frac{E_1}{G_{12}} - 2\nu_{21})\sin^2\alpha\cos^2\alpha]\}} \tag{5}$$

For a composite reinforced with the glass fabric with the parameters: $\alpha = 12^\circ$, $t_2 = 2t_1$ and elastic constants of a unidirectional material: longitudinal modulus, $E_1 = 60\,\mathrm{GPa}$, transverse modulus,

$E_2 = 13$ GPa, shear modulus, $G_{12} = 3.4$ GPa, Poisson's ratio $\nu_{21} = 0.3$, the modulus of elasticity $E_a = 23.5$ GPa. For comparison, a cross-ply $[0^\circ / 90^\circ]$ laminate made of the same material has $E = 36.5$ GPa [1]. Thus, the modulus of a woven structure is less by 37% than the modulus of the same material but reinforced with straight fibres.

The stiffness and strength of fabric composites depend not only on the yarns and matrix properties, but on material structural parameters as well, i.e. on fabric count and weave. The fabric count specifies the number of warp and fill yarns per inch, while the weave determines how the warp and the fill yarns are interlaced. Typical weave patterns are shown in Figure2 [1].

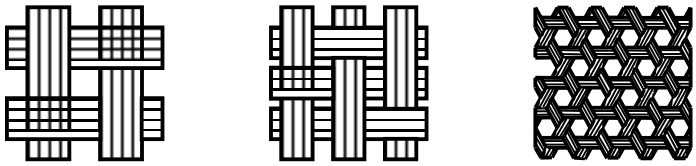

Figure 2. Plain (a), twill (b), and triaxial (c) woven fabrics

Various types of material models have been developed for the characterisation of fabric composites with these kinds of reinforcement [2-4].

Being formed from one and the same type of yarns plain, twill, and satin weaves provide approximately the same strength and stiffness of the fabric in the warp and the fill directions. Typical stress-strain diagrams for a fibreglass fabric composite of such a type are presented in Figure 3 [1]. As can be seen, material demonstrates relatively low stiffness and strength under tension at the angle of 45^0 with respect to the warp or fill directions. To improve these properties, multi-axial woven fabrics (one of this kind is shown in Figure 2(c)), can be used.

Fabric materials, whose properties are closer to those of unidirectional composites are made by weaving a great number of larger yarns in a longitudinal direction and fewer and smaller yarns in an orthogonal direction. Such a weave is called unidirectional. This provides materials with high stiffness and strength in one direction, which is specific for unidirectional composites, and high processability, typical for fabric composites.

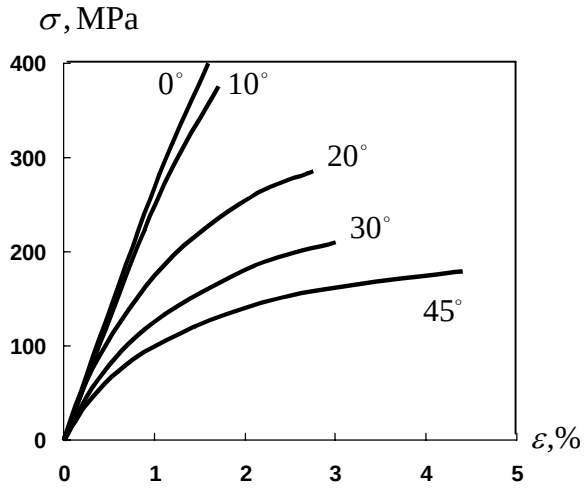

Figure 3. Stress-strain curves for fibreglass fabric composite loaded in tension at different angles with respect to the warp direction

Being fabricated as planar structures, fabrics can be shaped on shallow surfaces using the material's high stretching ability under tension at 45^0 to the yarns' directions.

Manufacturing of fabric-reinforced composite components with complex three-dimensional geometries needs the implementation of special kinds of technology including mapping between the two-dimensional fabric sheet and the three-dimensional surface, methods for predicting 'flattened' patterns used for fitting a sheet to a specific portion of the surface, techniques for inserting one or more 'darts' wherever necessary, methods for predicting and preventing defects such as wrinkling, folding, and tearing, and so on [5-6]. There are various approaches to the modelling the draping of woven fabrics onto complex geometries, namely the geometrical fitting, mechanical simulation of the drawing, and so on. The so-called fishnet analysis represents the first group, namely the geometrical fitting. In this

case the effect of material properties and interaction with tooling are not taken into account. The fabric is considered as a continuum sheet, and the analysis of the draping is effectively an extension of the deep drawing of metal forming processes for the second group of technologies [7]. A meso-structural modelling of the viscoelastic behaviour of resin combined with unidirectional non-linear elastic behaviour of warp and fill fibres during the shaping process belongs to the third group of methods that could be used as a part of the process design for fabric composite structures [8].
Much more possibilities for such shaping are provided by implementation of knitted fabrics whose strain to failure exceeds 100%. Moreover, a knitting process provides an opportunity to shape the fibrous preform in accordance with the shape of the future composite part.

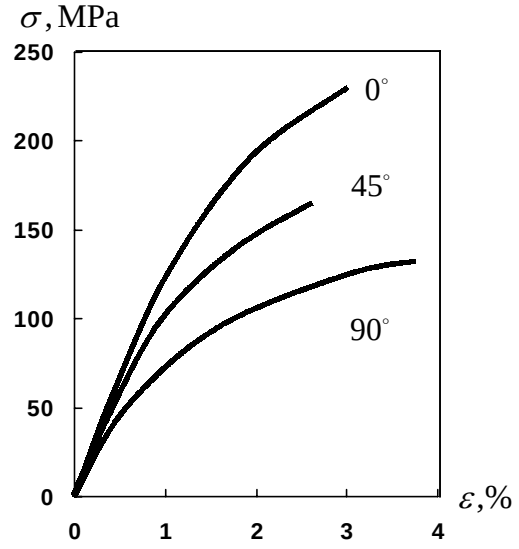

Figure 4. Typical stress-strain curves for fibreglass knitted composites loaded in tension at different angles with respect to the material structure primary orientation

Relatively high curvature of the yarns in knitted fabrics and possible fibre breakage in the process of knitting result in materials whose strength and stiffness are less than those of woven fabric composites, but whose processability is higher, and the cost is lower. Typical stress-strain diagrams for composites reinforced by knitted fabrics are presented in Figure 4 [1].
Material properties close to those of woven composites are provided by braided structures which, being usually tubular in form are fabricated by mutual intertwining, or twisting of yarns about each other. Typical braided structures are shown in Figure 5 [1].

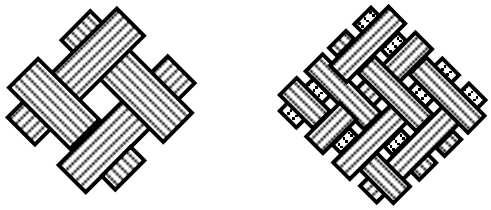

(*a*) (*b*)

Figure 5. Diamond (a) and regular (b) braided fabric structures

Biaxial braided fabrics in Figure 5 can incorporate longitudinal yarns forming a triaxial braid whose structure is similar to that shown in Figure 2 (d). Braided preforms are characterised with very high processability providing near net-shape manufacturing of tubes, and profiles with various cross-sectional shapes.
Fabric reinforced multilayer composites suits very well the manufacture of thin-walled structural components. Under the loading, however, delamination phenomena could occur at the interface between the individual layers due to the low interlaminar shear strength. One of the ways to improve this situation is the implementation of stitched textile composites. Additionally, this technology creates an opportunity to produce textile assembly of complex textile preforms and their further plastics processing. Examples of the fabric composite rotor production based on this technique could be found in [9].

In general, introduction of the out-of-plane reinforcement leads to the development of spatially reinforced composite structures. A natural way the spatial (3D) reinforcement is provided by implementation of three-dimensionally woven or braided fabrics. The similar results could be achieved using the aforementioned processes of sewing and stitching, needle punching, or introduction of short fibres (or whiskers). Another class of spatially reinforced composite materials is represented by bulk composites multi-dimensionally reinforced with fine rectilinear yarns composed from fibres bound with a matrix [10].

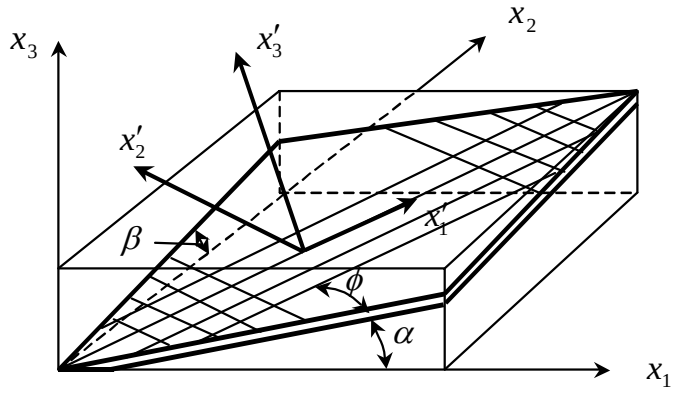

Figure 6. Spatial orientation of the fabric reinforcement

Special type of a spatial composite structure (see Figure 6) formed by the fabric composite in which the plies reinforced at angle ϕ (warp direction) with respect to the *x*-axis make angles α and β with the x_1-axis and the x_2-axis, respectively could be used for manufacture of thin-walled composite components [11]. This provides a possibility to design and manufacture thin-walled composite components with three-dimensional orientation of the fabric reinforcement and avoid the technological problems related to wrinkling, folding, tearing, etc.

3. MODELLING AND CHARACTERIZATION OF FABRIC COMPOSITES

Although a number of microstructural models of the type shown in Figure 1 and leading to equations similar to equation (5) have been developed to predict stiffness and even strength characteristics of fabric composites (e.g., [12]), for practical design and analysis, these characteristics are usually determined by experimental methods. Elastic constants entering constitutive equations written in the principal material coordinates, e.g. moduli of elasticity E_1, E_2, shear modulus G_{12}, and Poisson's ratios ν_{12}, ν_{21}, are found testing strips cut out of fabric composite plates at different angles with respect to the orthotropy axes. The 0° and 90° specimens are used to determine moduli of elasticity E_1, E_2 and Poisson's ratios ν_{12}, ν_{21} (or parameters of non-linear stress-strain diagrams), while the in-plane shear stiffness can be obtained with the aid of off-axis tensile test discussed in [1]. As shown in [1], there exists the angle of the reinforcement orientation ϕ^* specified by the following equation

$$\sin^2 \phi^* = \frac{\dfrac{1+\nu_{21}}{E_1} - \dfrac{1}{2G_{12}}}{\dfrac{1+\nu_{21}}{E_1} + \dfrac{1+\nu_{12}}{E_2} - \dfrac{1}{G_{12}}} \tag{6}$$

or

$$\sin^2 \phi^* = \frac{\dfrac{1+\nu_{yx}}{E_x} - \dfrac{1+\nu_{21}}{E_1}}{2\dfrac{1+\nu_{yx}}{E_x} - \dfrac{1+\nu_{21}}{E_1} - \dfrac{1+\nu_{12}}{E_2}} \tag{7}$$

such that off-axis tension under this angle is not accompanied with shear-extension coupling. For this angle shear modulus is found to be equal to

$$G_{12} = \frac{E_x}{2(1+\nu_{yx})} \tag{8}$$

where the modulus E_x and Poisson's ratio ν_{yx} are determined from the off-axis test performed on the specimen reinforced under angle ϕ^*.

For fabric composites whose stiffness in the warp and the fill directions is the same $(E_1 = E_2)$, equation (7) yields $\phi = 45^\circ$.

In general case the following equation could be used in order to find the shear modulus

$$G_{12} = \frac{\sin^2\phi\cos^2\phi}{\frac{1}{E_x} - \frac{\cos^4\phi}{E_1} - \frac{\sin^4\phi}{E_2} + \frac{2\nu_{21}}{E_1}\cos^2\phi} \tag{9}$$

This equation gives the value of the shear modulus corresponding ideal off-axis tensile test when the shear deformation of the specimen ends is not restrained. Applicability of this equation for the real test conditions is discussed in [1] in detail. As shown, reasonably fair results could be obtained for the specimens with $l > 3a$, where *l* is the length and *a* width of the specimen, and the angle $\phi = 10^\circ$. Thus, the uniaxial tensile test of the anisotropic flayer (off-axis test) can be used to obtain the in-plane shear modulus, G_{12}, while the other elastic constants entering constitutive equations written in the principal material coordinates could be determined from conventional tests performed on the standard specimens loaded in the direction of principal material axes.

Constitutive equations for the spatially reinforced composite material considered in previous section (see Figure 6.) are:

$$\{\sigma\} = [B]\{e\} - \{S\}t \tag{10}$$

where *t* is the temperature change. Stiffness, B_{ijlk}, and thermal, S_{ij}, coefficients are calculated in terms of the mechanical and physical properties of the elementary layers as follows

$$B_{ijlk} = B'_{i'j'k'l'} l_{ij'} l_{ji'} l_{kl'} l_{lk'}; \qquad S_{ij} = B'_{i'j'k'l'} l_{ij'} l_{ji'} \alpha'_{k'l'}$$

where, according to Figure 6 directional cosines are:

$$l_{11} = \cos\lambda\cos\psi; \quad l_{12} = -\sin\lambda\cos\psi; \quad l_{13} = -\sin\psi;$$

$$l_{21} = \sin\lambda\cos\beta - \sin\beta\sin\psi\cos\lambda;$$

$$l_{22} = \cos\lambda\cos\beta + \sin\beta\sin\lambda\sin\psi; \quad l_{23} = -\sin\beta\cos\psi;$$

$$l_{31} = \sin\lambda\sin\beta + \cos\lambda\cos\beta\sin\psi;$$

$$l_{32} = \sin\beta\cos\lambda - \cos\beta\sin\lambda\sin\psi; \quad l_{33} = \cos\beta\cos\psi;$$

$$\psi = \tan^{-1}(\tan\alpha\cos\beta); \quad \lambda = \phi + \tan^{-1}(\sin\psi\tan\beta); \tag{11}$$

The tensor components of the elastic constants $B'_{i'j'k'l'}$ and the coefficients of linear thermal expansion $\alpha'_{k'l'}$ for the elementary fabric layer referred to the system of coordinates x'_1, x'_2, x'_3 are expressed in terms of moduli of elasticity E_1, E_2, E_3 shear moduli G_{12}, G_{13}, G_{23}, Poisson's ratios ν_{12}, ν_{13}, ν_{23}, and coefficients of linear expansion α_1, α_2, α_3 [13-14]. Additional tests are required, in order to determine transverse characteristics of the fabric reinforced composite and complete the material mechanical characterisation in this case.

4. SPATIAL STRUCTURES FORMED BY FABRIC COMPOSITES

As discussed in Section 3, a considerable improvement of the composite laminate properties in transverse direction could be achieved if the material is additionally reinforced with fibres or yarns in the direction orthogonal (or making some angles) to the layer plane. Various technological developments have been implemented in this area including stitched textile assemblies, three-dimensional weaving or braiding, needle punching, spatial multi-dimensional composite reinforcement, etc. [2-4, 10-11].
Similar results could be achieved implementing the special type of a spatial composite structure (see Figure 6) assembled from the spatially oriented fabric layers and using the helical lay-up method [11]. Lightweight thin-walled components (usually with the rotational shapes and geometries) could be designed and fabricated on the basis of this technology. General approach to the modelling and analysis of the thin-walled composite shells reinforced in this way has been developed in [13]. This approach takes into account anisotropic characteristics of the material (due to the three-dimensional layer orientation), additional structural parameters (angles of the layer orientation), and a three-dimensional stress state of an elementary layer.

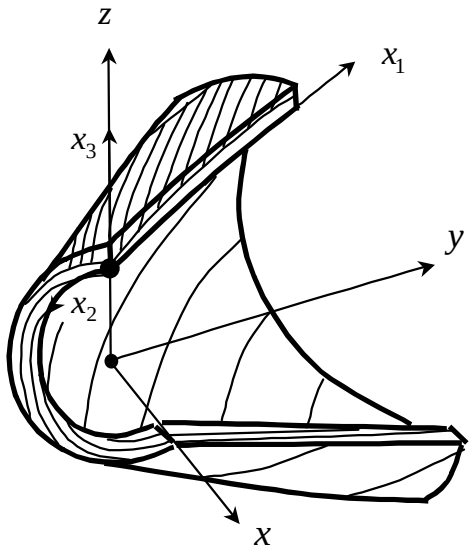

Figure 7. Spatially reinforced shell of revolution

Based on this theory, the analysis of axisymmetrical shell of revolution (see Figure 7) is discussed in this paper in order to demonstrate basic features of the mechanical behaviour, typical for the composite structures with the specified above type of reinforcement.
The constitutive equations for the shell presented in Figure 7 have the form

$$\{N\} = h\left[\overline{B}_{mn}\right]\begin{Bmatrix}\varepsilon\\ \psi\end{Bmatrix} - \{T\}_0, \qquad m=1,\ldots,3;\ n=1,\ldots,5$$

$$\{M\} = \frac{h^3}{12}\left[\overline{B}_{mn}\right]\{\kappa\} - \{T\}_1, \quad m,n=1,\ldots,3 \tag{12}$$

$$\{Q\} = \left[I_{pq}\right]\begin{Bmatrix}\varepsilon\\ \psi\end{Bmatrix} - \{I\}_t, \qquad p=1,\ldots,2;\ \ q=1,\ldots,5$$

where $\{N\} = \{N_1, N_2, N_{12}\}^T$, $\{M\} = \{M_1, M_2, M_{12}\}^T$, and $\{Q\} = \{Q_1, Q_2\}^T$ are the vectors of stress resultants, bending moments, and transverse shear stress resultants respectively; $\begin{Bmatrix}\varepsilon\\ \psi\end{Bmatrix} = \{\varepsilon_1, \varepsilon_2, \varepsilon_{12}, \psi_1, \psi_2\}^T$ is the vector of strains $\varepsilon_1, \varepsilon_2, \varepsilon_{12}$ and transverse shear strains ψ_1, ψ_2;

$\{\kappa\} = \{\kappa_1, \kappa_2, \kappa_{12}\}^T$ is the vector of variables induced by bending and torsion of the shell element $\{T\}_0 = \{T_1^{(0)}, T_2^{(0)}, T_{12}^{(0)}\}^T$, $\{T\}_1 = \{T_1^{(1)}, T_2^{(1)}, T_{12}^{(1)}\}^T$, $\{I\}_t = \{I_{t1}, I_{t2}\}^T$ are the vectors of thermal coefficients; *h* is the total thickness of the shell [15].

The generalized stiffness coefficients $\overline{B}_{mn}$ in the Eqns. (12) are linked with the stiffness characteristics B_{ijlk} in the following way

$$\overline{B}_{m1} = B_{mm11};\quad \overline{B}_{m2} = B_{mm22};\quad \overline{B}_{m3} = B_{mm12};\quad \overline{B}_{m4} = B_{mm13};\quad \overline{B}_{m5} = B_{mm23} \qquad (m = 1,\ldots,3)$$

The components of the vectors of thermal coefficients are determined as:

$$T_1^{(k)} = \int_{-h/2}^{h/2} (S_{11}t - B_{1111}e_1^t - B_{1122}e_2^t - B_{1112}e_{12}^t)x_3^k dx_3$$

$$T_2^{(k)} = \int_{-h/2}^{h/2} (S_{22}t - B_{2222}e_2^t - B_{2211}e_1^t - B_{2221}e_{21}^t)x_3^k dx_3$$

$$T_{12}^{(k)} = \int_{-h/2}^{h/2} [S_{12}t - 2(B_{1211}e_1^t + B_{1222}e_2^t + 2B_{1212}e_{12}^t)x_3^k dx_3, \qquad (k = 0, 1)$$

The coefficients I_{pq}, I_{tq} ($p = 1,\ldots,2$; $q = 1,\ldots,5$) are presented by the following equations [14]

$$I_{1m} = K_1(\nu_{13,23}U_m - V_m), \qquad m = 1,\ldots,3$$

$$I_{14} = K_1(1 + \nu_{13,23}U_4 - V_4), \qquad I_{15} = K_1[\nu_{13,23}(U_5 - 1) - V_5]$$

$$I_{1n} = K_2(\nu_{23,13}V_n - U_n), \qquad n = 1,\ldots,3$$

$$I_{24} = K_2[\nu_{23,13}(V_4 - 1) - U_4], \qquad I_{25} = K_2(1 - U_5 + \nu_{23,13}V_5) \qquad (13)$$

$$I_{t1} = \frac{K_1}{h}\int_{-h/2}^{h/2} \left\{\nu_{13,23}[(U_t + \alpha_{23})t - U_1e_1^t - U_2e_2^t] - [(V_t + \alpha_{13})t - V_1e_1^t - V_2e_2^t]\right\} dx_3$$

$$I_{t2} = \frac{K_2}{h}\int_{-h/2}^{h/2} \left\{\nu_{23,13}[(V_t + \alpha_{23})t - V_1e_1^t - V_2e_2^t] - [(U_t + \alpha_{23})t - U_1e_1^t - U_2e_2^t]\right\} dx_3$$

where *t* is the temperature change, and

$$U_m = \frac{\eta_{23,1}}{E_1}\overline{B}_{1m} + \frac{\eta_{23,2}}{E_2}\overline{B}_{2m} + \frac{\nu_{23,12}}{G_{12}}\overline{B}_{3m}, \qquad m = 1,\ldots,5,t$$

$$V_n = \frac{\eta_{13,1}}{E_1}\overline{B}_{1n} + \frac{\eta_{13,2}}{E_2}\overline{B}_{2n} + \frac{\nu_{13,12}}{G_{12}}\overline{B}_{3n}, \qquad n = 1,\ldots,5,t$$

$$K_1 = hG_{13}/(1 - \nu_{23,31}\nu_{13,23}), \qquad K_2 = hG_{23}/(1 - \nu_{13,23}\nu_{23,13})$$

$$(\overline{B}_{1t} = S_{11},\ \overline{B}_{1t} = S_{22},\ \overline{B}_{3t} = S_{12})$$

Elastic constants E_1, E_2, G_{12}, $\nu_{ij,kl}$, $\eta_{ij,k}$, and coefficients of thermal deformation α_3, α_{13}, α_{23} are calculated in terms of the same set of constants of the elementary fabric layers and the angles of layer orientation as the coefficients B_{ijlk} [13-14].

Thermal strain components for the shell of revolution with the axis of rotation *y* (see Figure 7) are presented in the following form

$$e_1^t = \frac{u_3^t}{R_1} - \frac{1}{A_1}\frac{du_1^t}{dy}, \quad e_2^t = \frac{u_3^t}{R_2} - \frac{u_1^t}{A_1 A_2}\frac{dr}{dy}, \quad e_{12}^t = 0 \tag{14}$$

where $A_1 = \sqrt{1+(dr/dy)^2}$, $A_2 = r(y)$, *r(y)* is the function specifying the shape of the shell meridian, and R_1, R_2 are the two principal curvature radii $R_1 = -\left[1+(dr/dy)^2\right]^{3/2}/(d^2r/d^2y)$, $R_2 = r\sqrt{1+(dr/dy)^2}$.

Thermal components of the displacements have the form [14]:

$$u_1^t = \frac{1}{A_1}\int_0^{x_3}\frac{du_3^t}{dy}dx_3, \qquad u_2^t = 0, \qquad u_3^t = \int_0^{x_3}\alpha_3 t dx_3 \tag{15}$$

Complete model of the spatially reinforced composite shell of revolution under consideration should also be supplemented with the appropriate strain-displacement relationships and equilibrium equations [15].

4.1 Example

Implementation of the aforementioned spatial fabric reinforcement with three-dimensional orientation leads to the substantial improvement in the transverse properties of the composite wall of structural component. At the same time, transverse interlaminar properties of the composite material itself (even oriented under three angles) still could deliver the problems due to possible delamination failure. Therefore, it is essential to know what would be the transverse normal and shear stresses acting at the level of elementary fabric layer. In this paper the case of thermal loading of the thin-walled shell made from a composite with carbon matrix is considered. The shell is reinforced with the patterns of the carbon fabric (see Figure 7) and subjected to the heating up to the temperature of 1000 K as part of the processing procedure. According to this technology, the wall of the shell is heated up uniformly over the thickness. The shell is placed vertically and resting at one end on the floor with the freedom to expand in radial directions. The relevant material property data for the particular design example considered in this study are as follows: $E_1' = 1.9\cdot10^4$ MPa, $E_2' = 8000$ MPa, $E_3' = 5000$ MPa, $G_{12}' = 4000$ MPa, $G_{13}' = 5000$ MPa, $G_{23}' = 5000$ MPa, ν'_{21}=0.15, $\nu'_{13}=\nu'_{23}$ =0.2 $\alpha_1' = 2\cdot10^{-6}$ 1/K, $\alpha_2' = 3.6\cdot10^{-6}$ 1/K, $\alpha_3' = 5\cdot10^{-6}$ 1/K. The geometry and angles of reinforcement orientation $\alpha(y)$, $\phi(y)$ are shown in Figure 8.

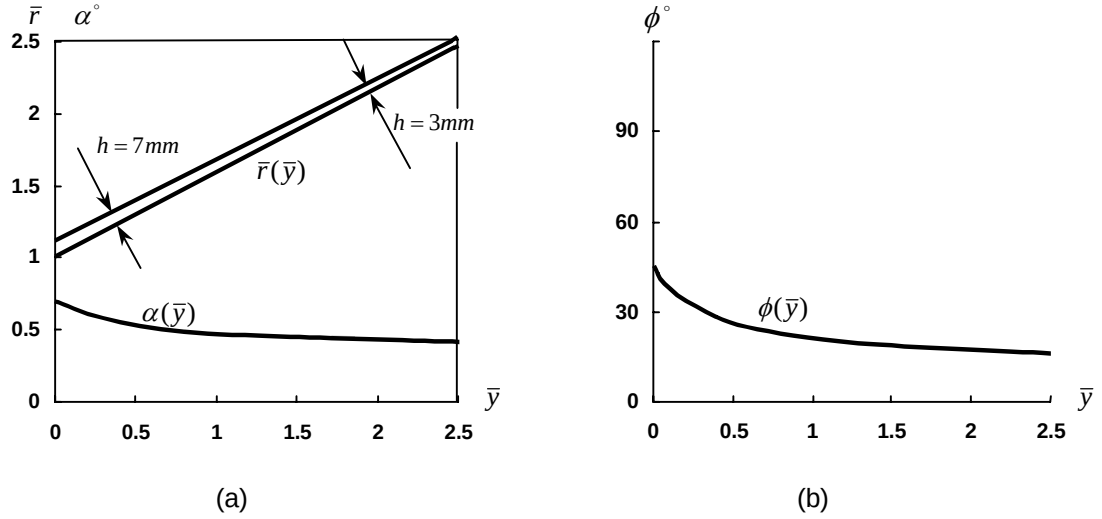

(a) (b)

Figure 8. Shape of the shell and the angles of reinforcement orientation ($\bar{y} = y/y_0$, $\bar{r} = r/r_0$)

The angle $\beta(y)$ has been calculated as:

$$\beta = \sin^{-1}\left[\delta\left(\delta^2 + \frac{4\pi^2 r^2}{N^2}\right)^{-1/2}\right]$$

where, *N* is the number of the fabric patterns composing the shell and δ is the thickness of the elementary fabric layer [14]. For the shell under consideration $N = 180$ and $\delta = 0.25\,\mathrm{mm}$.

The stress and strain analysis has been performed on the basis of membrane theory of shell and accordingly the bending moments and shear forces were taken equal to zero: $M_1 = M_2 = M_{12} = Q_1 = Q_2 = 0$ in equations (12). Furthermore, the membrane stress resultants and thermal terms $T_1^{(1)}$, $T_2^{(1)}$, $T_{12}^{(1)}$ were also equal to zero, $N_1 = N_2 = N_{12} = 0$, since there were no any mechanical loads applied and temperature has been distributed uniformly over the thickness of the wall. As a result the second group of the equations (12) yields $\kappa_1 = \kappa_2 = \kappa_{12} = 0$. Solution of the five linear equations left after this rearrangement determines the distribution of strain components ε_1, ε_2, ε_{12}, ψ_1, ψ_2 (see Figure9). The strain in the transverse direction (across the wall thickness) is calculated as $\varepsilon_3 = \alpha_3 t$.

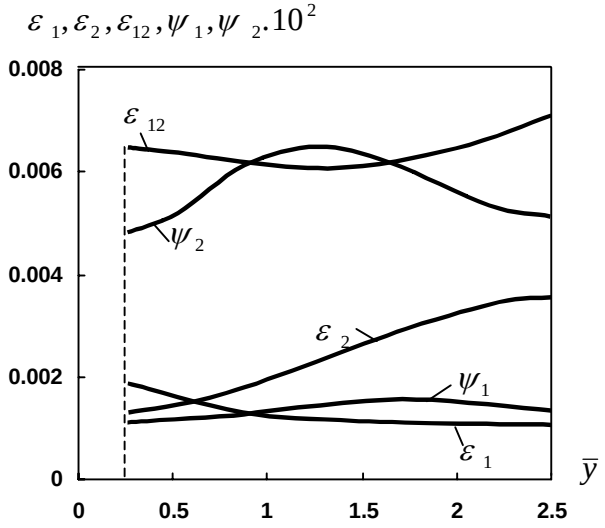

Figure 9. Strain distributions

The strains of the elementary composite layer ε_1', ε_2', ε_{12}' are calculated in terms of the strains of the shell ε_1, ε_2, ε_{12}, ψ_1, ψ_2 using a coordinate transformation from the coordinates (x_1, x_2, x_3) to coordinates (x_1', x_2', x_3'). Corresponding stresses σ_1', σ_2', τ_{12}' are found using equations of the generalized Hooke's law written for the elementary fabric layer. In order to calculate transverse stress σ_3 and transverse shear stresses τ_{13}, τ_{23}, the three dimensional equilibrium equations of the theory of elasticity referred to the corresponding orthogonal curvilinear coordinate frame should be integrated, taking into account static boundary conditions at the inner surface of the shell [14]:

$$\tau_{13} = -\frac{1}{A_1 A_2}\int_{-h/2}^{x_3}\left(\frac{d(r\sigma_1)}{dy} - \sigma_2\frac{dr}{dy}\right)dx_3, \quad \tau_{23} = -\frac{1}{A_1 A_2^2}\int_{-h/2}^{x_3}\frac{d(A_2^2\tau_{12})}{dy}dx_3 \qquad (16)$$

$$\sigma_3 = -\frac{1}{A_1 A_2}\int_{-h/2}^{x_3}\left[\frac{d(A_2\tau_{13})}{dy} + \frac{r(d^2r/dy^2)}{1+(dr/dy)^2}\sigma_1 - \sigma_2\right]dx_3 - A_1 A_2 p$$

Here stresses σ_1, σ_2, τ_{12} are calculated in terms of the shell strains as follows:

$$\sigma_1 = \overline{B}_{11}(\varepsilon_1 + x_3\kappa_1) + \overline{B}_{12}(\varepsilon_2 + x_3\kappa_2) + \overline{B}_{13}(\varepsilon_{12} + x_3\kappa_{12}) + \overline{B}_{14}\psi_1 + \overline{B}_{15}\psi_2$$
$$-(\overline{B}_{1t}t - \overline{B}_{11}e_{1t} - \overline{B}_{12}e_{2t} - \overline{B}_{13}e_{12t}),$$

$$\sigma_2 = \overline{B}_{21}(\varepsilon_1 + x_3\kappa_1) + \overline{B}_{22}(\varepsilon_2 + x_3\kappa_2) + \overline{B}_{23}(\varepsilon_{12} + x_3\kappa_{12}) + \overline{B}_{24}\psi_1 + \overline{B}_{25}\psi_2 - (\overline{B}_{2t}t - \overline{B}_{21}e_{1t} - \overline{B}_{22}e_{2t} - \overline{B}_{23}e_{12t}),$$

$$\tau_{12} = \overline{B}_{31}(\varepsilon_1 + x_3\kappa_1) + \overline{B}_{32}(\varepsilon_2 + x_3\kappa_2) + \overline{B}_{33}(\varepsilon_{12} + x_3\kappa_{12}) + \overline{B}_{34}\psi_1 + \overline{B}_{35}\psi_2 - (\overline{B}_{3t}t - \overline{B}_{31}e_{1t} - \overline{B}_{32}e_{2t} - \overline{B}_{33}e_{12t}). \quad (17)$$

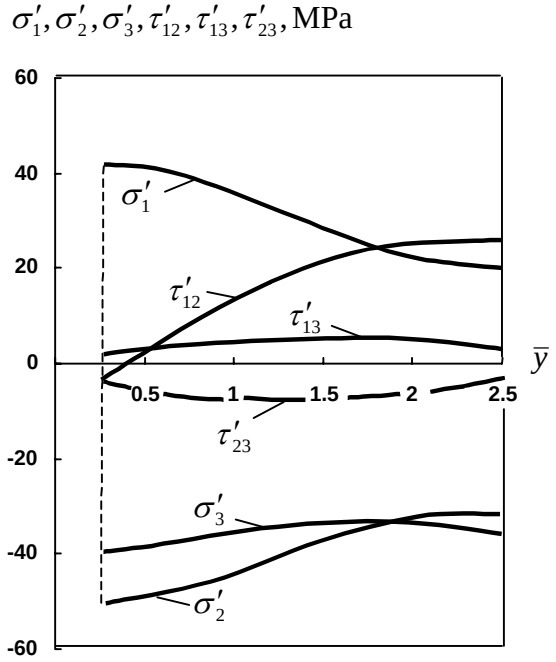

Figure 10. Stress distributions in the elementary fabric layers

The corresponding transverse stresses σ_3', τ_{13}', τ_{23}' acting in the elementary fabric layers are calculated using the stress transformation relations.
Results of stress calculation are shown in Figure 10. As can be seen, the normal transverse stresses σ_3' are compressive and the values of transverse shear stresses τ_{13}', τ_{23}' are relatively low ($\tau_{13}' \le 6\,\text{MPa}$, $\tau_{23}' \le 8\,\text{MPa}$). This justifies the viability of the structure under consideration, since the transverse strength of the laminated material is substantially higher in compression compared to tensile strength, which is determined primarily by the tensile strength of the matrix. Thus an advantage of the spatial three-dimensional orientation of the fabric reinforcement can be taken in this case, preserving at the same time a reasonable level of the material resistance to the delamination mode of failure.

5. SUMMARY

This paper has presented developments in the modelling and characterisation of fabric reinforced composite materials and considered a particular application of spatial fabric reinforcement to the design and manufacture of composite thin-walled structures. The corresponding material and structural mechanical models are discussed in conjunction with the implementation of a helical lay-up manufacturing technology to the fabrication of the spatially reinforced rotational thin-walled components. The spatial structure of the material has been determined by the three angles of the fabric layer (pattern) orientation: ϕ (warp direction), α and β (see Figure 6). The shell of revolution is composed from the fabric patterns placed onto mould or mandrel reproducing a spatial helical surface. The stress analysis was performed for the case of uniform heating of the shell conducted as a part of processing procedure, typical for the fabrication of composite components with carbon matrix. It was found that the normal transverse stresses σ_3' are compressive ($\sigma_{3compr}' \le 40\,\text{MPa}$) and the values

of transverse shear stresses τ'_{13}, τ'_{23} acting in the elementary fabric layers are reasonably low ($\tau'_{13} \le 6\,\mathrm{MPa}$, $\tau'_{23} \le 8\,\mathrm{MPa}$), compared to the corresponding strength parameters of the laminated composite. This creates an opportunity to avoid delaminations of the material at the processing stage of the shell and provides conditions for maintaining the structural integrity under operational loads.

6. CONCLUSION

The material and structural models discussed in this paper could be implemented for stress analysis of thin-walled structures composed from the spatially oriented fabric layers in the aforementioned manner for given operational conditions.

REFERENCES

1. *V.V. Vasiliev and E.V. Morozov. Mechanics and Analysis of Composite Materials. (2001), Elsevier Science.*
2. *A.E. Bogdanovich and C.M. Pastore. Mechanics of Textile and Laminated Composites. (1996), Chapman & Hall.*
3. *T.W. Chou and F.K. Ko (Eds). Textile Structural Composites. (1989), Elsevier Science.*
4. *N.K. Niranjan. Woven Fabric Composites. (1994), Lancaster, Pa., Technomic.*
5. *M. Aono. Computer-Aided Geometric Design for Forming Woven Cloth Composites. PhD Thesis. (1994), Design and Manufacturing Institute, Rensselaer Polytechnic Institute, Troy, New York.*
6. *B.P. Van West and S.C. Luby. Fabric draping simulation in composites manufacturing. Part I and II. J. Adv. Materials (April 1997), pp. 29-41.*
7. *L.Dong, C. Lekakou and M.G. Bader. Solid mechanics draping simulations of woven fabrics. Proc. of the 12th International Conference on Composite Materials (ICCM-12), Paris, France, (July 1999), (CD-ROM).*
8. *J.L.Billoet, and A. Cherouat. Meso-structural behaviour of composite fabric for the simulation of manufacturing of thin composite by shaping process. Proc. of the 12th International Conference on Composite Materials (ICCM-12), Paris, France, (July 1999), (CD-ROM).*
9. *C. Herzberg, S. Krzywinski and H. Rodel. Load-adapted 3D-reinfircement through function-adjusted stitching technique. Proc. of the 13th International Conference on Composite Materials (ICCM-13), Beijing, China, (June 2001), (CD-ROM).*
10. *Yu.M. Tarnopol'skii, I.G. Zhigun and V.A. Polyakov. Spatially Reinforced Composites. (1992), Technomic, PA.*
11. *N.J. Pagano and L.E. Whitford. On the solution for the elastic response of involute bodies. Composite Sci. Technol. 22(4), (1985), pp. 295-317.*
12. *A.M. Skudra, F.Ya. Bulavs, M.R. Gurvich and A.A. Kruklinsh. Elements of Structural Mechanics of Composite Truss Systems. (1989), Riga, Zinatne (in Russian).*
13. *V.V.Vasiliev and E.V. Morozov. Applied theory of spatially reinforced composite shells. J. of Mechanics of Composite Materials, Vol.24, No.3, (1988). N.Y.: Plenum Publishing Corp., pp. 393-400.*
14. *V.V. Vorobey, E.V. Morozov, and O.V. Tatarnikov, Analysis of Thermostressed Composite Structures. (1992), Moscow, Mashinostroenie (in Russian).*
15. *E.V. Morozov. Analysis of spatially reinforced composite shells of revolution. Proc. of the 13th International Conference on Composite Materials (ICCM-13), Beijing, China, (June 2001), (CD-ROM).*

∇Δ